

Rydberg states of muonic helium in quantum electrodynamics

A. V. Eskin,¹ A. P. Martynenko,¹ F. A. Martynenko,¹ and D. K. Pometko¹

¹*Samara University, Samara, Russia*

The variational method is used to study the energy levels of muonic helium ($\mu^- - e^- - He$) with an electron in the ground state and a muon in an excited state with principal and orbital quantum numbers $n \sim l + 1 \sim 14$. The variational wave functions are chosen in the Gaussian form. The matrix elements of the Hamiltonian in the nonrelativistic approximation, as well as corrections for the vacuum polarization and relativism, are calculated analytically. A series of energies of the Rydberg muon states is obtained, which can be studied experimentally.

I. INTRODUCTION

The Rydberg states in atoms play an important role in refining the values of fundamental constants. For example, measurements of the Rydberg constant [1, 2] have been improved using the Rydberg state spectroscopy in the hydrogen atom. Working with the Rydberg states can reduce the influence of strong interaction corrections on the energy level structure. The electron Rydberg atoms are characterized by very low ionization energies and have characteristic sizes that increase as n^2 [3] compared to the ground state size. Since the radiative lifetime of the excited state is proportional to n^3 , the Rydberg atoms are characterized by extremely long lifetimes: from a thousandth of a second to one second. Using the method of stepwise photoexcitation with tunable lasers, the Rydberg atoms with principal quantum numbers $n \sim 1000$ have been obtained. The low density of matter in the interstellar medium and, consequently, the low probability of collisional ionization, determine the long lifetimes of the Rydberg atoms in space. Electromagnetic radiation from the Rydberg atoms makes it possible to determine the composition and characteristics of a matter in the interstellar medium. Thus, the Rydberg atoms of hydrogen with $n > 150$ and carbon with $n > 700$ were discovered using radiation lines in the radio range in outer space.

In the paper [4], the Rydberg levels of the hydrogen atom in an electric field were studied. The Lamb shift-based measurement of the proton charge radius r_p in muonic hydrogen atom yields a smaller value than the measurement of r_p in ordinary hydrogen. This discrepancy

is known as the "proton radius puzzle" [5, 6]. r_p is found indirectly from measurements of the Rydberg constant R , where the electron wave function partially overlaps with the proton volume, and a correlation between r_p and R should exist. Therefore, experiments with highly excited Rydberg states, which are sensitive to R but have little effect on r_p , are important for resolving the r_p problem. However, such measurements would require very high frequency resolution. In the work [4], this difficulty was overcome by studying hydrogen in an electric field. Transitions to the Rydberg states (with a known correction for the Stark effect) with quantum numbers $n = 20$ and $n = 24$ were measured, and the ionization energy was found. The Rydberg frequency cR was obtained using a method insensitive to r_p . The result [4] confirms the value of r_p obtained in the experiment with muonic hydrogen and contributes to a more accurate resolution of the r_p problem. It can be said quite definitely that, along with the study of low-lying energy levels [7] in the hydrogen atom, the study of highly excited states is of considerable interest for a more precise determination of a number of physical parameters of the theory with high accuracy.

The aim of this work is to investigate the Rydberg states in muon-electron helium atoms with excited muon states in which the muon and electron are approximately equidistant from the nucleus. When a beam of negative muons enters a helium target, it is slowed to a kinetic energy of several tens of eV due to ionization and excitation of target molecules. An exotic muonic helium atom is formed when a muon stops within the target and is captured by the target atom into an outer atomic orbit, replacing one of the electrons in an orbit with $n \leq 14$. The capture is a complex process and depends on the atomic and molecular structure, the range of values of the principal quantum number n , and the angular momentum l . The lifetime of a muonic helium atom is determined by large orbital angular momentum of $l = (10 \div 13)$, at which point the muon is formed. Its transition to the ground state with $l = 0$ is strongly suppressed. The lifetime of such an atom is a few nanoseconds. After capture, the muon cascades from its excited Rydberg state through the atom's own series of bound states, located within the electron levels due to its greater mass. The cascade is accompanied by the emission of X-rays and ends when the particle is absorbed by the nucleus as a result of the weak interaction. The muon cascades downward through the Coulomb deexcitation and external Auger emission until the probability of radiative transitions becomes dominant for lower-lying states. The cascade time in an exotic muonic helium atom is short compared to the particle lifetime, making X-ray processes observable

using spectroscopic methods. In the case of muonic Rydberg states in muonic helium, the influence of nuclear structure effects on the emission spectrum is significantly reduced. For pionic helium atoms, studies of the Rydberg states allow us to obtain a more accurate pion mass than is known from other sources [8–10]. M. Hori’s group plans to perform laser spectroscopy of the kaonic atom using the kaon beam at DAPHNE, which will improve the accuracy of charged kaon mass determination by 2-3 orders of magnitude compared to the current level.

It is worth noting that other approaches to determining the π -meson mass exist. A study conducted in [11] demonstrates the potential of crystal spectroscopy of exotic atoms. In this work, the $5g - 4f$ transitions in pion nitrogen and muon oxygen were measured simultaneously in a gaseous nitrogen-oxygen mixture. Knowing the muon mass, the muon line can be used to energy-calibrate the pion transition. The obtained mass of the negatively charged pion is 4.2 ppm higher than the current world average of 139.57077 ± 0.00017 MeV [12].

The energy levels of three-particle systems can be studied with high accuracy using the variational method. There are some differences in the use of the variational method for finding the energy levels of three-particle systems. These differences relate to the choice of coordinates and the representation of the Hamiltonian to describe the system, as well as the choice of basis wave functions. Thus, in the work [8], an exponential basis was used, and the coordinates of the electron and muon were determined relative to the nucleus. In the works [13, 14], when calculating the energy levels of hydrogen mesomolecules, muonic helium, and other molecules, we use the formulation of the variational method in the Jacobi coordinates with the Gaussian wave functions in the case of three-particle and four-particle systems. Using this approach, we calculated the energy levels of the Rydberg states in pion and kaonic helium atoms [15, 16]. In this paper, we extend the scope of research to muonic helium atoms ($\mu^- - e^- - He$) and perform energy level calculations for states in which the muon is in an excited state with a large orbital quantum number $l = 10, 11, 12, 13$.

II. GENERAL FORMALISM

Various approaches have been developed to study the energy levels of three-particle systems. One method, analytical perturbation theory, allows for analytical investigation of

both the Lamb shift and the hyperfine structure of the spectrum [17–23]. Other methods used for many-particle systems are the variational method and the hyperspherical coordinate method, which allow for very high-precision determination of the energy levels and wave functions of bound states. [24–34]. Since the muonic helium system considers atomic states with large muon orbital angular momenta, where the electron and muon are equidistant from the nucleus, it is virtually impossible to use analytical perturbation theory. Therefore, we further study this system using the variational method. Gaussian wave functions are used as basis wave functions.

To find the energy levels of a three-particle system, we introduce the Jacobi coordinates $\boldsymbol{\rho}$, $\boldsymbol{\lambda}$, connected with the radius vectors of the particles \mathbf{r}_1 (nucleus), \mathbf{r}_2 (muon), \mathbf{r}_3 (electron) as follows:

$$\boldsymbol{\rho} = \mathbf{r}_2 - \mathbf{r}_1, \quad \boldsymbol{\lambda} = \mathbf{r}_3 - \frac{m_1\mathbf{r}_1 + m_2\mathbf{r}_2}{m_1 + m_2}, \quad (1)$$

where m_1 , m_2 , m_3 are the masses of the He nucleus, muon and electron.

To solve the variational problem, we choose the wave functions of the ground state in the form of a superposition of Gaussian exponentials:

$$\Psi(\boldsymbol{\rho}, \boldsymbol{\lambda}, A) = \sum_{i=1}^K C_i \psi_i(\boldsymbol{\rho}, \boldsymbol{\lambda}, A^i), \quad \psi_i(\boldsymbol{\rho}, \boldsymbol{\lambda}, A^i) = e^{-\frac{1}{2}(A_{11}^i \boldsymbol{\rho}^2 + 2A_{12}^i \boldsymbol{\rho} \boldsymbol{\lambda} + A_{22}^i \boldsymbol{\lambda}^2)}, \quad (2)$$

where C_i are the linear variational parameters, A^i is the matrix of nonlinear variational parameters, K is the size of the basis.

In the non-relativistic approximation, the Hamiltonian of a three-particle atom in Jacobi coordinates can be represented as:

$$\hat{H}_0 = -\frac{1}{2\mu_1} \nabla_{\boldsymbol{\rho}}^2 - \frac{1}{2\mu_2} \nabla_{\boldsymbol{\lambda}}^2 + \frac{e_1 e_2}{|\boldsymbol{\rho}|} + \frac{e_1 e_3}{|\boldsymbol{\lambda} + \frac{m_2}{m_{12}} \boldsymbol{\rho}|} + \frac{e_2 e_3}{|\boldsymbol{\lambda} - \frac{m_1}{m_{12}} \boldsymbol{\rho}|}, \quad (3)$$

where $m_{12} = m_1 + m_2$, $\mu_1 = \frac{m_1 m_2}{m_1 + m_2}$, $\mu_2 = \frac{(m_1 + m_2) m_3}{m_1 + m_2 + m_3}$, e_1 , e_2 , e_3 are the charges of the helium nucleus, muon, and electron.

For arbitrary states of a muon and an electron with orbital angular momenta l_1 and l_2 , a convenient basis for expanding functions that depend on angles is the bipolar spherical harmonics [35]:

$$[Y_{l_1}(\theta_{\rho}, \phi_{\rho}) \otimes Y_{l_2}(\theta_{\lambda}, \phi_{\lambda})]_{LM} = \sum_{m_1, m_2} C_{l_1 m_1 l_2 m_2}^{LM} Y_{l_1 m_1}(\theta_{\rho}, \phi_{\rho}) Y_{l_2 m_2}(\theta_{\lambda}, \phi_{\lambda}), \quad (4)$$

where θ_ρ, ϕ_ρ and $\theta_\lambda, \phi_\lambda$ are the spherical angles that determine the direction of the vectors $\boldsymbol{\rho}$ and $\boldsymbol{\lambda}$, $C_{l_1 m_1 l_2 m_2}^{LM}$ are the Clebsch-Gordon coefficients. Since in muonic helium the μ^- meson is in an excited state with orbital angular momentum l , and the electron is in the ground state, the variational wave function of the system is chosen as:

$$\Psi_{lm}(\boldsymbol{\rho}, \boldsymbol{\lambda}, A) = \sum_{i=1}^K C_i Y_{lm}(\theta_\rho, \phi_\rho) \rho^l e^{-\frac{1}{2}(A_{11}^i \rho^2 + 2A_{12}^i \boldsymbol{\rho} \boldsymbol{\lambda} + A_{22}^i \lambda^2)}, \quad (5)$$

where the spherical function $Y_{lm}(\theta_\rho, \phi_\rho)$ describes the angular part of the muon's orbital motion. Within the variational approach, solving the Schroedinger equation reduces to solving the following matrix problem for the coefficients C_i :

$$H \cdot C = EB \cdot C, \quad (6)$$

where the matrix elements of the Hamiltonian H_{ij} and the normalization B_{ij} can be calculated analytically in the basis of Gaussian wave functions. Thus, the normalization of the wave function (5) is determined by the following expression:

$$\langle \Psi | \Psi \rangle = \sum_{i,j=1}^K C_i C_j 2^{l+2} \pi^{\frac{3}{2}} \Gamma\left(l + \frac{3}{2}\right) \frac{B_{22}^l}{(\det B)^{l+\frac{3}{2}}}, \quad B_{kn} = A_{kn}^i + A_{kn}^j, \quad (7)$$

where $\Gamma(l + \frac{3}{2})$ is the Euler gamma function.

Let's consider other analytical results for the Hamiltonian matrix elements. The kinetic energy operator contains two terms. The matrix element of the Laplace operator with respect to $\boldsymbol{\lambda}$ is:

$$\langle \Psi | \nabla_{\boldsymbol{\lambda}}^2 | \Psi \rangle = \sum_{i,j=1}^K \frac{C_i C_j 2^{l+2} \pi^{\frac{3}{2}}}{\langle \Psi | \Psi \rangle} \Gamma\left(l + \frac{3}{2}\right) \frac{B_{22}^{l-1}}{(\det B)^{l+\frac{3}{2}}} \times [3A_{22}^i (A_{22}^i - B_{22}) \det B + (2l+3)(A_{22}^i B_{12} - A_{12}^i B_{22})^2]. \quad (8)$$

A similar matrix element with the Laplace operator on $\boldsymbol{\rho}$ is also expressed through non-linear variational parameters as follows:

$$\langle \Psi | \nabla_{\boldsymbol{\rho}}^2 | \Psi \rangle = \sum_{i,j=1}^K \frac{C_i C_j 2^{l+1} \pi^{\frac{3}{2}}}{\langle \Psi | \Psi \rangle} \Gamma\left(l + \frac{1}{2}\right) \frac{B_{22}^{l-1}}{(\det B)^{l+\frac{3}{2}}} \times [(2l+1) \det B (- (2l+3) A_{11}^i B_{22} + 3(A_{12}^i)^2 + 2l A_{12}^i B_{12}) + (2l+1)(2l+3)(A_{12}^i B_{12} - A_{11}^i B_{22})^2]. \quad (9)$$

The potential energy operator in the nonrelativistic Hamiltonian consists of pairwise Coulomb interactions U_{ij} ($i, j=1, 2, 3$). The matrix elements of the potential energy (in

electron atomic units) are represented by compact expressions for arbitrary states with muon orbital angular momentum l :

$$\langle \Psi | U_{12} | \Psi \rangle = -Z \sum_{i,j=1}^K \frac{C_i C_j 2^{l+\frac{3}{2}} \pi^{\frac{3}{2}}}{\langle \Psi | \Psi \rangle} \Gamma(l+1) \frac{B_{22}^{l-1}}{(\det B)^{l+1}}, \quad (10)$$

$$\langle \Psi | U_{13} | \Psi \rangle = -Z \sum_{i,j=1}^K \frac{C_i C_j 2^{l+\frac{5}{2}} \pi}{\langle \Psi | \Psi \rangle} \Gamma\left(l + \frac{3}{2}\right) \frac{B_{22}^{l+\frac{1}{2}}}{(\det B)^{l+\frac{3}{2}}} {}_2F_1\left(\frac{1}{2}, l + \frac{3}{2}, \frac{3}{2}, -\frac{(F_2^{23})^2}{\det B}\right) \quad (11)$$

$$\langle \Psi | U_{23} | \Psi \rangle = \sum_{i,j=1}^K \frac{C_i C_j 2^{l+\frac{5}{2}} \pi}{\langle \Psi | \Psi \rangle} \Gamma\left(l + \frac{3}{2}\right) \frac{B_{22}^{l+\frac{1}{2}}}{(\det B)^{l+\frac{3}{2}}} {}_2F_1\left(\frac{1}{2}, l + \frac{3}{2}, \frac{3}{2}, -\frac{(F_2^{13})^2}{\det B}\right) \quad (12)$$

$$F_2^{13} = B_{12} + \frac{m_1}{m_{12}} B_{22}, \quad F_2^{23} = B_{12} - \frac{m_2}{m_{12}} B_{22}, \quad (13)$$

where ${}_2F_1(\alpha, \beta, x)$ is the hypergeometric function.

For $l = 1$, expressions (10)-(12) coincide with the previously obtained results [13]. Using the matrix elements of the Hamiltonian \hat{H}_0 , some energy levels of muonic helium ($\mu^- e^- He$) are calculated in the Matlab system. The calculations are performed using our program, which was previously used to calculate the energy levels of three- and four-particle atoms in quantum electrodynamics [14–16]. The calculation results are shown in Table I.

To improve the accuracy of our calculations, we take into account several important corrections to the Hamiltonian \hat{H}_0 . The pairwise electromagnetic interaction between particles in quantum electrodynamics is determined by the Breit potential [36]. Among the various terms of this potential, we highlight those terms with the greatest numerical value. These include relativistic corrections, contact interactions, and corrections for vacuum polarization.

Relativistic corrections are defined in the energy spectrum by the following terms in electron atomic units (e.a.u.):

$$\Delta U_{rel} = -\frac{\alpha^2}{8} \left(\frac{\mathbf{p}_1^4}{m_1^3} + \frac{\mathbf{p}_2^4}{m_2^3} + \frac{\mathbf{p}_3^4}{m_3^3} \right). \quad (14)$$

The main contribution to the relativistic correction (14) is connected with the electron's motion. The value of the corresponding matrix element from ΔU_{rel}^e can be obtained in exactly the same way as (8) in terms of variational parameters:

$$\langle \Psi | -\frac{\alpha^2}{8} \nabla_{\lambda}^4 | \Psi \rangle = -\alpha^2 \sum_{i,j=1}^K \frac{C_i C_j 2^{l-1} \pi^{\frac{3}{2}}}{\langle \Psi | \Psi \rangle} \Gamma\left(l + \frac{3}{2}\right) \frac{B_{22}^{l-2}}{(\det B)^{l+\frac{7}{2}}} \left[15(A_{22}^i)^2 (\det B)^2 (A_{22}^i - B_{22})^2 + \right. \quad (15)$$

TABLE I: Energy levels of the Rydberg states of muonic helium obtained in the non-relativistic approximation and the values of the main corrections in the energy spectrum in electron atomic units (e.a.u.).

State	E_{nr}	$-\frac{\alpha^2}{8}\mathbf{p}_e^4$	ΔU_{vp}	ΔU_{cont}
(${}^3_2\text{He} - \mu^- - e^-$) atom				
(14,13)	-2.8111108864	-0.0003033020	-0.0000003281	0.0000036145
(14,12)	-2.8428981924	-0.0003199814	-0.0000003462	0.0000038048
(13,12)	-3.0709070711	-0.0002521330	-0.0000002833	0.0000030296
(13,11)	-3.1015704843	-0.0002756076	-0.0000003043	0.0000032420
(12,11)	-3.4261731529	-0.0002051832	-0.0000002424	0.0000024722
(12,10)	-3.4584490501	-0.0001933630	-0.0000002334	0.0000023297
(${}^4_2\text{He} - \mu^- - e^-$) atom				
(14,13)	-2.8250592886	-0.0003018206	-0.0000003257	0.0000036074
(14,12)	-2.8567044908	-0.0003153649	-0.0000003420	0.0000037043
(13,12)	-3.0887395538	-0.0001946102	-0.0000002337	0.0000024480
(13,11)	-3.1191663050	-0.0002763101	-0.0000002931	0.0000030883
(12,11)	-3.4485457935	-0.0001980560	-0.0000002398	0.0000024205
(12,10)	-3.4818179188	-0.0002111030	-0.0000002456	0.0000023483

$$10(2l+3)A_{22}^i(A_{22}^i - B_{22})\det B(A_{22}^i B_{12} - A_{12}^i B_{22})^2 + (2l+3)(2l+5)(A_{22}^i B_{12} - A_{12}^i B_{22})^4].$$

We also take into account the effects of vacuum polarization in the energy spectrum. Since the Compton wavelength of both the electron and the muon in a highly excited state is much smaller than the radius of the Bohr orbit, we can use the following expression for the vacuum polarization potential in e.a.u.:

$$\Delta U_{vp} = \Delta U_{vp}(r_{13}) + \Delta U_{vp}(r_{23}) = -\frac{4}{15}\alpha^2(Z\alpha)\delta(\boldsymbol{\lambda} + \frac{m_2}{m_{12}}\boldsymbol{\rho}) + \frac{4}{15}\alpha^2(Z\alpha)\delta(\boldsymbol{\lambda} - \frac{m_1}{m_{12}}\boldsymbol{\rho}). \quad (16)$$

The matrix elements of such potentials are calculated analytically using (2) in closed form:

$$\langle \Psi | \Delta U_{vp}(r_{13}) | \Psi \rangle = -\frac{4}{15}\alpha^2(Z\alpha) \sum_{i,j=1}^K \frac{C_i C_j 2^{l+\frac{1}{2}}}{\langle \Psi | \Psi \rangle} \Gamma\left(l + \frac{3}{2}\right) \frac{1}{(F_1^{13})^{l+\frac{3}{2}}}, \quad (17)$$

$$\langle \Psi | \Delta U_{vp}(r_{23}) | \Psi \rangle = -\frac{4}{15} \alpha^2 (Z\alpha) \sum_{i,j=1}^K \frac{C_i C_j 2^{l+\frac{1}{2}}}{\langle \Psi | \Psi \rangle} \Gamma\left(l + \frac{3}{2}\right) \frac{1}{(F_1^{23})^{l+\frac{3}{2}}}, \quad (18)$$

$$F_1^{13} = B_{11} + \frac{m_2^2}{m_{12}^2} B_{22} - 2 \frac{m_2}{m_{12}} B_{12}, \quad F_1^{23} = B_{11} + \frac{m_1^2}{m_{12}^2} B_{22} + 2 \frac{m_1}{m_{12}} B_{12}. \quad (19)$$

The contact interaction potential, like (16), is expressed through δ -functions in the form (in electron atomic units):

$$\Delta U_{cont} = \frac{\pi Z \alpha^2}{2} \delta\left(\boldsymbol{\lambda} + \frac{m_2}{m_{12}} \boldsymbol{\rho}\right) - \frac{\pi \alpha^2}{2} \delta\left(\boldsymbol{\lambda} - \frac{m_1}{m_{12}} \boldsymbol{\rho}\right). \quad (20)$$

Table I presents the results of calculating the energy values using the Hamiltonian \hat{H}_0 and the values of the matrix elements (15), (17), (18), (20).

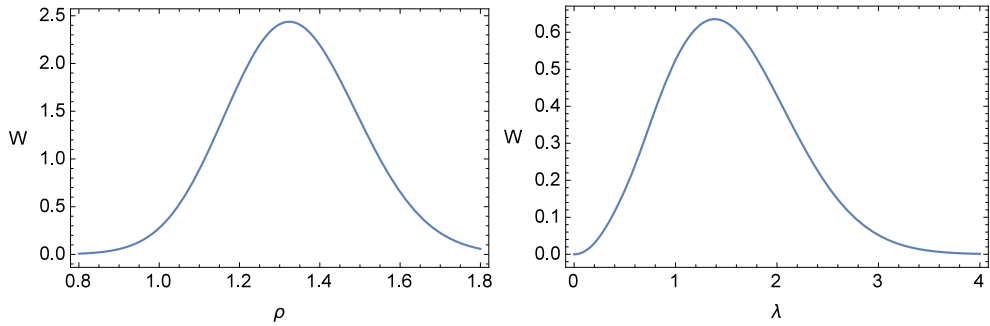


FIG. 1: Radial distribution densities $W(\rho)$, $W(\lambda)$ for the (14, 13) state of $(\frac{4}{2}He - \mu^- - e^-)$. The values of the variables ρ and λ are expressed in electron atomic units.

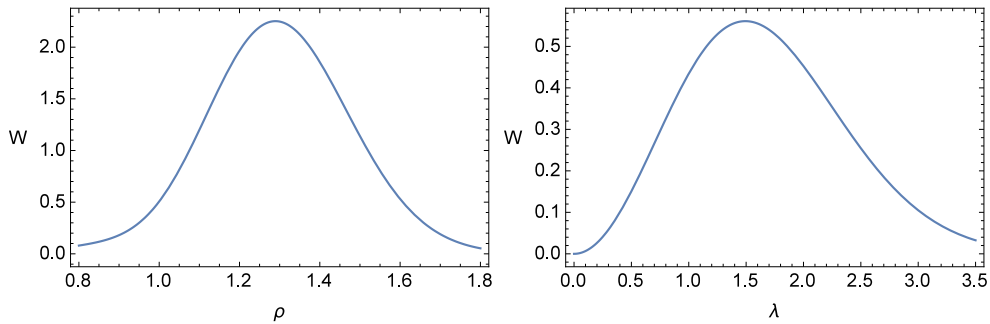


FIG. 2: Radial distribution densities $W(\rho)$, $W(\lambda)$ for the (13, 12) state of $(\frac{4}{2}He - \mu^- - e^-)$. The values of the variables ρ and λ are expressed in electron atomic units.

To study the internal structure of three-particle bound states, we calculate the mean-square distances between particles. The corresponding matrix elements are calculated analytically, and the results are presented in Appendix A. Using the relations (A1)-(A3),

we present the numerical values of the mean-square distances between particles in the (${}^4\text{He} - \mu^- - e^-$) atom for the (14, 13) state, numbering the particles as follows: $\text{He} \rightarrow 1$, $\mu^- \rightarrow 2$, $e^- \rightarrow 3$:

$$\delta_{12} = \sqrt{\langle (\mathbf{r}_1 - \mathbf{r}_2)^2 \rangle} = 1.34 (0.71 \times 10^{-8} \text{ cm}), \quad (21)$$

$$\delta_{13} = \sqrt{\langle (\mathbf{r}_1 - \mathbf{r}_3)^2 \rangle} = 0.47 (0.25 \times 10^{-8} \text{ cm}), \quad (22)$$

$$\delta_{23} = \sqrt{\langle (\mathbf{r}_2 - \mathbf{r}_3)^2 \rangle} = 1.08 (0.57 \times 10^{-8} \text{ cm}). \quad (23)$$

Average distances between particles are presented in (21)-(23) in electron atomic units and in cm (in parentheses).

Some details of the internal structure of bound states can also be obtained by constructing the radial distribution densities for ρ and λ and calculating the root-mean-square values of $\langle \rho^2 \rangle$, $\langle \lambda^2 \rangle$, which are determined by the expressions:

$$W(\rho) = \frac{(2\pi)^{\frac{3}{2}}}{\langle \Psi | \Psi \rangle} \sum_{i,j=1}^K \frac{C_i C_j}{B_{22}^{3/2}} \rho^{(2l+2)} e^{-\frac{1}{2} \frac{\det B}{B_{22}} \rho^2}, \quad (24)$$

$$W(\lambda) = \frac{2^{l+\frac{5}{2}} \pi}{\langle \Psi | \Psi \rangle} \sum_{i,j=1}^K \frac{C_i C_j \Gamma(l + \frac{3}{2})}{B_{11}^{l+\frac{3}{2}}} \lambda^2 e^{-\frac{1}{2} B_{22} \lambda^2} {}_1F_1 \left(l + \frac{3}{2}, \frac{3}{2}, \frac{B_{12}^2 \lambda^2}{2B_{11}} \right), \quad (25)$$

$$W(\rho, \lambda) = \frac{4\pi}{\langle \Psi | \Psi \rangle} \sum_{i,j=1}^K \frac{C_i C_j}{B_{12}} \rho^{2l+1} \lambda e^{-\frac{1}{2} [B_{11} \rho^2 + B_{22} \lambda^2]} sh(B_{12} \rho \lambda), \quad B_{lk} = A_{lk}^i + A_{lk}^j, \quad (26)$$

$$\langle \rho^2 \rangle = \frac{\pi^{\frac{3}{2}} 2^{l+3} \Gamma(l + \frac{5}{2})}{\langle \Psi | \Psi \rangle} \sum_{i,j=1}^K C_i C_j \frac{B_{22}^{l+1}}{(\det B)^{l+5/2}}, \quad (27)$$

$$\langle \lambda^2 \rangle = \frac{\pi^{\frac{3}{2}} 2^{l+2} \Gamma(l + \frac{3}{2})}{\langle \Psi | \Psi \rangle} \sum_{i,j=1}^K C_i C_j \frac{B_{22}^{l-1}}{(\det B)^{l+\frac{5}{2}}} (3B_{11} B_{22} + 2B_{12}^2 l). \quad (28)$$

The radial distribution densities are shown in Figs. 1 and 2 for muonic helium-4. These graphs demonstrate the presence of characteristic distances in three-particle systems (${}^3, {}^4\text{He} - \mu^- - e^-$). From the graphs in Figs. 1 and 2, it follows that for the states under consideration, the muon is located at approximately the same distances from the nucleus as the electron. The distribution densities for the two radial variables, rho and lambda, provide a more complete picture of the characteristic distances in this three-particle system. They are shown in Fig. 3.

Note that we do not consider the fine splitting in a three-particle atom, determined by the interaction of the electron spin and the large orbital angular momentum of the muon.

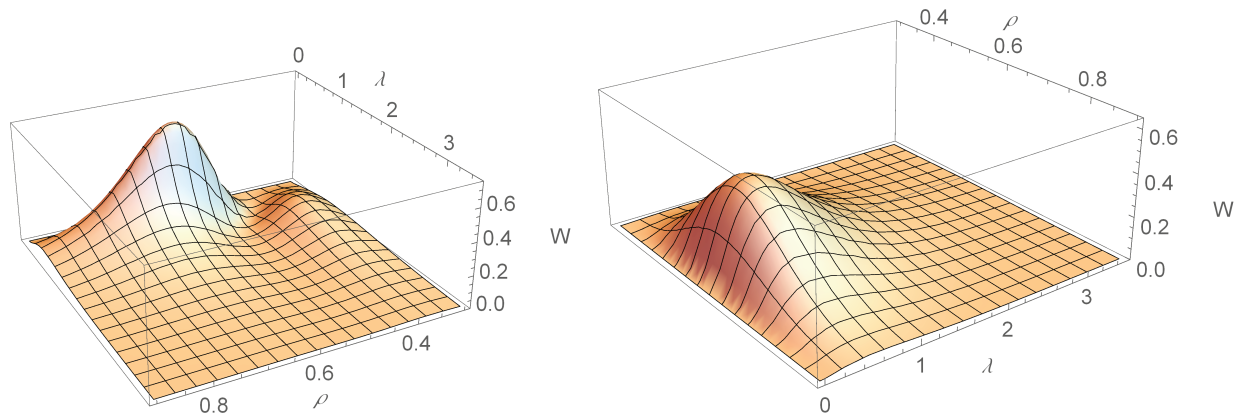


FIG. 3: Radial distribution density $W(\rho, \lambda)$ for the states (14,13) ($\mu^- - e^- -^4 He$) and (14,12) ($\mu^- - e^- -^3 He$). The values of the variables ρ and λ are expressed in electron atomic units.

III. CONCLUSION

A field of research in physics has recently emerged devoted to studying the properties of exotic atoms [37–39]. These include a wide variety of systems. These atoms have short lifetimes, but they also have a relatively simple structure (two-particle and three-particle), allowing for the use in their study of rigorous methods and the calculation of observable properties with a high degree of accuracy. Experiments conducted with these atoms allow us to take a look into the field of particle interactions inaccessible to conventional systems. Spectroscopy of various exotic atoms and molecules can provide new information about the nature of fundamental interactions and the values of fundamental parameters of the Standard Model. For example, the PiHe collaboration performed laser spectroscopy of the infrared transition in three-particle pion helium atoms [8, 9]. These atoms were created in a superfluid (He-II) helium target. Similar measurements in antiproton helium atoms embedded in liquid helium were performed by the CERN ASACUSA collaboration [40]. As a result of such experiments, it is possible to determine a more precise ratio of the masses of the antiproton and electron, and the pion and electron. A similar program for studying kaonic helium is planned for a more accurate measurement of the K-meson mass.

The exotic atom of muonic helium ($\mu^- - e^- - He$) is formed by the capture of a negative muon by the helium atom as a result of electromagnetic interaction. It should be noted that research into muonic, pionic, and kaonic helium, as well as the various processes connected with their formation, has been underway for quite some time. Initially, a beam

of muons (pions, kaons) slows down in matter. Once a muon reaches a state in which its kinetic energy is zero, it is captured by an atom and transitions to states with high orbital angular momentum, forming a muonic atom. The exact distribution of these states is unknown experimentally. Since all low-lying muonic states are unoccupied, the muon quickly transitions to the lowest accessible quantum state (1S). Auger and radiative transitions are responsible for this de-excitation. The study of muonic helium was fraught with various technical and scientific difficulties, including the availability of intense muon beams, accurate X-ray spectroscopy, and effective analysis of the background radiation. It can be said that these difficulties have been largely overcome. The measured energies of the $(n,l)-(1s)$ transitions in the case of $(\mu^- - He^{++})$ with $n \leq 6$ have been obtained in many studies and are in good agreement with theoretical estimates. The emitted radiation for transitions to the lowest-lying levels is in the X-ray energy range.

In this work, we investigate excited states in neutral muonic helium, a system that exhibits similarities to the muonic helium ion but is clearly distinct from it [41–46]. Therefore, a detailed comparison of our numerical results with previous calculations for neutral muonic helium proved difficult due to the virtual absence of such calculations. We calculate the energy levels of high-lying orbits that overlap significantly with the electron shells of the atom. These orbits are characterized by a principal quantum number $n \sim 14$. The studied principal quantum number distributions in [41] confirm this well. Measurements of the X-ray intensity of such high-level transitions (as well as Auger transitions), when compared with muon cascade calculations, provide information on the initial population of muonic states with quantum numbers (n, l) . In this way, information is obtained regarding the probabilities of atomic muon capture, which is determined by the fraction of particles that are localized in helium atoms by replacing valence electrons.

We study the energy levels of muonic helium for states in which the muon has such a large orbital angular momentum that it is approximately at the same distance from the nucleus as the electron. Calculations are performed in leading order using the variational method with a Gaussian basis, and several key corrections determined by the Breit Hamiltonian (relativism, vacuum polarizations and contact interactions) are calculated in first-order perturbation theory. Since the electron is in the 1S state, the three-particle state in Table I is denoted by (n, l) , where l is the muon's orbital angular momentum and n is the principal quantum number of the $(\mu^- He^{++})$ subsystem.

Our previous studies of the energy levels of both pionic and kaonic helium were performed within the variational approach developed in [15, 16]. An important addition to our previous studies is the calculation of the energy levels of excited states of muonic helium, which is performed in this paper. The numerical results obtained in Table I can be used in parallel to analyze experimental data for both pionic helium and muonic helium, and measuring the transition frequencies between Rydberg states in muonic helium opens a new opportunity for determining the muon mass.

Acknowledgments

The authors are grateful to V.I. Korobov for helpful discussions. This work was supported by the Russian Science Foundation (grant no. RSF 25-72-00029) (F.A.M.).

Appendix A: Root mean square distances between particles.

To calculate the mean-square distances between particles, we use the explicit form of the wave function of the system (2). The results of the analytical integration are as follows:

$$\langle(\mathbf{r}_1 - \mathbf{r}_2)^2\rangle = \sum_{I,J=1}^K \frac{C_I C_J}{\langle\Psi|\Psi\rangle} 2^{(l+3)} \pi^{\frac{3}{2}} \Gamma(l + \frac{5}{2}) \frac{B_{22}^{(l+1)}}{(\det B)^{(l+\frac{5}{2})}}, \quad (\text{A1})$$

$$\langle(\mathbf{r}_1 - \mathbf{r}_2)^2\rangle = \sum_{I,J=1}^K \frac{C_I C_J}{\langle\Psi|\Psi\rangle} 2^{(l+2)} \pi^{\frac{3}{2}} \Gamma(l + \frac{3}{2}) \frac{B_{22}^{(l-1)}}{(\det B)^{(l+\frac{5}{2})}} \left[(2l+3) \left(B_{12} - \frac{m_2}{m_{12}} B_{22} \right)^2 + 3 \det B \right], \quad (\text{A2})$$

$$\langle(\mathbf{r}_2 - \mathbf{r}_3)^2\rangle = \sum_{I,J=1}^K \frac{C_I C_J}{\langle\Psi|\Psi\rangle} 2^{(l+2)} \pi^{\frac{3}{2}} \Gamma(l + \frac{3}{2}) \frac{B_{22}^{(l-1)}}{(\det B)^{(l+\frac{5}{2})}} \left[(2l+3) \left(B_{12} + \frac{m_1}{m_{12}} B_{22} \right)^2 + 3 \det B \right], \quad (\text{A3})$$

Using the general formulas (A1)-(A3) one can obtain numerical values of the average

distances between particles.

-
- [1] B. de Beauvoir, F. Nez, L. Julien, et al., Absolute Frequency Measurement of the 2S-8S/D Transitions in Hydrogen and Deuterium: New Determination of the Rydberg Constant, *Phys. Rev. Lett.* **78**, 440 (1997); <https://doi.org/10.1103/PhysRevLett.78.440>.
- [2] C. Schwob, L. Jozefowski, B. de Beauvoir, et al., Optical Frequency Measurement of the 2S-12D Transitions in Hydrogen and Deuterium: Rydberg Constant and Lamb Shift Determinations, *Phys. Rev. Lett.* **82**, 4960 (1999); <https://doi.org/10.1103/PhysRevLett.82.4960>.
- [3] T. F. Gallagher, *Rydberg atoms*, Cambridge University Press, NY, 1994.
- [4] S. Scheidegger and F. Merkt, Precision-spectroscopic determination of the binding energy of a two-body quantum system: The hydrogen atom and the proton-size puzzle, *Phys. Rev. Lett.* **132**, 113001 (2024); <https://doi.org/10.1103/PhysRevLett.132.113001>.
- [5] A. Antognini, F. Hagelstein, V. Pascalutsa, The proton structure in and out of muonic hydrogen, *Ann. Rev. Nucl. Part. Sci.* **72**, 389 (2022); <https://doi.org/10.1146/annurev-nucl-101920-024709>.
- [6] U. D. Jentschura and D. C. Yost, Precision Rydberg state spectroscopy with slow electrons and the proton-radius puzzle, *Phys. Rev. A* **108**, 062822 (2023); <https://doi.org/10.1103/PhysRevA.108.062822>.
- [7] M. I. Eides, H. Grotch and V. A. Shelyuto, Theory of light hydrogenlike atoms, *Phys. Rept.* **342**, 63 (2001); [https://doi.org/10.1016/S0370-1573\(00\)00077-6](https://doi.org/10.1016/S0370-1573(00)00077-6).
- [8] M. Hori, A. Soter, V. I. Korobov, Proposed method for laser spectroscopy of pionic helium atoms to determine the charged-pion mass, *Phys. Rev. A* **89**, 042515 (2014); <https://doi.org/10.1103/PhysRevA.89.042515>.
- [9] M. Hori, H. Aghai-Khozani, A. S3ter, A. Dax, D. Barna, Laser spectroscopy of pionic helium atoms, *Nature* **581**, 37 (2020); <https://doi.org/10.1038/s41586-020-2240-x>.
- [10] D. Bakalov and B. Obreshkov, Collisional shift and broadening of the transition lines in pionic helium, *Phys. Rev.* **93**, 062505 (2016); <https://doi.org/10.1103/PhysRevA.93.062505>.
- [11] M. Trassinelli, D. F. Anagnostopoulos, G. Borchert et al., Measurement of the charged pion mass using X-ray spectroscopy of exotic atoms, *Phys. Lett. B* **759**, 583 (2016); <https://doi.org/10.1016/j.physletb.2016.06.025>.

- [12] S. Navas et al. (Particle Data Group), Review of Particle Physics, Phys. Rev. D **110**, 030001 (2024); <https://doi.org/10.1103/PhysRevD.110.030001>.
- [13] A. V. Eskin, V. I. Korobov, A. P. Martynenko and F. A. Martynenko, Energy Levels of Three-Particle Muon Electron Helium in Variational Approach, Phys. Atom. Nucl. **86**, 4, 583 (2023); <https://doi.org/10.1134/S106377882304021X>.
- [14] A. V. Eskin, A. P. Martynenko, F. A. Martynenko, D. K. Pometko, Few-particle lepton bound states in variational approach, arXiv:2602.10068[hep-ph] (2026); <https://arxiv.org/abs/2602.10068v2>.
- [15] V. I. Korobov, F. A. Martynenko, A. P. Martynenko, and A. V. Eskin, Energy Levels of Pionic and Kaonic Helium in the Variational Approach, Phys. Part. Nucl. **55**, 4, 705 (2024); <https://doi.org/10.1134/S1063779624700047>.
- [16] V. I. Korobov, A. V. Eskin, A. P. Martynenko, F. A. Martynenko, Energy levels of mesonic helium in quantum electrodynamics, Phys. Rev. A **109**, 3, 032802 (2024); <https://doi.org/10.1103/PhysRevA.109.032802>.
- [17] S. D. Lakdawala and P. Mohr, Hyperfine structure in muonic helium, Phys. Rev. A **22**, 1572 (1980); <https://doi.org/10.1103/PhysRevA.22.1572>.
- [18] K. N. Huang and V. W. Hughes, Theoretical hyperfine structure of the muonic ${}^3\text{He}$ and ${}^4\text{He}$ atoms, Phys. Rev. A **26**, 2330 (1982); <https://doi.org/10.1103/PhysRevA.26.2330>.
- [19] M. Ya. Amusia, M. Ju. Kuchiev, V. L. Yakhontov, Computation of the hyperfine structure in the $(\alpha - \mu^- - e^-)^0$ atom, J. Phys. B **16**, L71 (1983); <https://doi.org/10.1088/0022-3700/16/3/007>.
- [20] S. G. Karshenboim, V. G. Ivanov, M. Ya. Amusia, Lamb shift of electronic states in neutral muonic helium, an electron-muon-nucleus system, Phys. Rev. A **91**, 3, 032510 (2015); <https://doi.org/10.1103/PhysRevA.91.032510>.
- [21] A. A. Krutov and A. P. Martynenko, Ground-state hyperfine structure of the muonic helium atom, Phys. Rev. A **78**, 032513 (2008); <https://doi.org/10.1103/PhysRevA.78.032513>.
- [22] R. N. Faustov, V. I. Korobov, A. P. Martynenko, F. A. Martynenko, Ground-state hyperfine structure of light muon-electron ions, Phys. Rev. A **105**, 042816 (2022); <https://doi.org/10.1103/PhysRevA.105.042816>.
- [23] A. E. Dorokhov, V. I. Korobov, A. P. Martynenko, F. A. Martynenko, Low-lying electron energy levels in three-particle electron-muon ions of Li, Be, and B, Phys. Rev. A **103**, 052806

- (2021); <https://doi.org/10.1103/PhysRevA.103.052806>.
- [24] R. J. Drachman, Nobrelativistic hyperfine splitting in muonic helium by adiabatic perturbation theory, *Phys. Rev. A* **22**, 1755 (1980); <https://doi.org/10.1103/PhysRevA.22.1755>.
- [25] S. I. Vinitsky, V. S. Melezhik, I. I. Ponomarev et al., Calculation of Energy Levels of Hydrogen Isotope μ Mesic Molecules in the Adiabatic Representation of Three-body Problem, *Sov. Phys. JETP* **52**, 353 (1980).
- [26] M. Puchalski, D. Kedziera, and K. Pachucki, Ground state of Li and Be^+ using explicitly correlated functions, *Phys. Rev. A* **80**, 032521 (2009); <http://dx.doi.org/10.1103/PhysRevA.80.032521>.
- [27] M. Puchalski and K. Pachucki, Applications of four-body exponentially correlated functions, *Phys. Rev. A* **81**, 052505 (2010); <http://dx.doi.org/10.1103/PhysRevA.81.052505>.
- [28] A. M. Frolov, Properties and hyperfine structure of helium-muonic atoms, *Phys. Rev. A* **61**, 022509 (2000); <https://doi.org/10.1103/PhysRevA.61.022509>.
- [29] A. M. Frolov, The hyperfine structure of the ground states in the helium-muonic atoms, *Phys. Lett. A* **376**, 2548 (2012); <http://dx.doi.org/10.1016/j.physleta.2012.06.024>.
- [30] M.-K. Chen, Correlated wave functions and hyperfine splitting of the 2s state of muonic 3,4He atoms, *Phys. Rev. A* **45**, 3, 1479 (1992); <https://doi.org/10.1103/PhysRevA.45.1479>.
- [31] H. Fatehizadeh, R. Gheisari, H. Falinejad, Full calculation of μpd and μdt muonic bound levels: Combination of Nikiforov-Uvarov method and variational approach, *Ann. Phys.* **385**, 512 (2017); <https://doi.org/10.1016/j.aop.2017.07.017>.
- [32] K. Varga and Y. Suzuki, Solution of few-body problems with the stochastic variational method I. Central forces with zero orbital momentum, *Comp. Phys. Comm.* **106**, 157 (1997); [https://doi.org/10.1016/S0010-4655\(97\)00059-3](https://doi.org/10.1016/S0010-4655(97)00059-3).
- [33] V. I. Korobov, Variational Methods in the Quantum Three-Body Problem with Coulomb Interaction, *Phys. Part. Nucl.* **53**, No. 1, 5 (2022); <https://doi.org/10.1134/S1063779622010038>.
- [34] Md. A. Khan, Hyperspherical three-body calculation for exotic atoms, *Few-Body Syst.* **52**: 53-63 (2012); <https://doi.org/10.1007/s00601-011-0264-3>.
- [35] D. A. Varshalovich, V. K. Khersonsky, E. V. Orlenko, and A. N. Moskalev, Quantum theory of angular momentum and its applications, Vol. I, M., Fizmatlit, 2017.
- [36] L. D. Landau and E. M. Lifshitz, Course of Theoretical Physics, Vol. 4: Quantum Electrodynamics, Fizmatlit, M., 2008; Pergamon, NY, 1977, 3rd ed.

- [37] N. C. Mukhopadhyay, Nuclear Muon capture, Phys. Rep. **30**, No.1, pp.1-144 (1977); [https://doi.org/10.1016/0375-9474\(80\)90172-4](https://doi.org/10.1016/0375-9474(80)90172-4).
- [38] F. Scheck, Muon Physics, Phys. Rep. **44**, No.4, pp.187-248 (1978); [https://doi.org/10.1016/0370-1573\(78\)90014-5](https://doi.org/10.1016/0370-1573(78)90014-5).
- [39] C. Curceanu, C. Guaraldo, M. Iliescu, et al., The modern era of light kaonic atom experiments, Rev. Mod. Phys. **91**, 025006 (2019); <https://doi.org/10.1103/RevModPhys.91.025006>.
- [40] A. Sóter, H. Aghai-Khozani, D. Barna, A. Dax, L. Venturelli and M. Hori, High-resolution laser resonances of antiprotonic helium in superfluid ^4He , Nature **603**, 411 (2022); <https://doi.org/10.1038/s41586-022-04440-7>.
- [41] J. S. Cohen, Multielectron effects in capture of antiprotons and muons by helium and neon, Phys. Rev. A **62**, 022512 (2000); <https://doi.org/10.1103/PhysRevA.62.022512>.
- [42] R. Landua and E. Klempt, Atomic Cascade of Muonic and Pionic Helium Atoms, Phys. Rev. Lett. **48**, 1722 (1982); <https://doi.org/10.1103/PhysRevLett.48.1722>.
- [43] S. Baird, C. J. Batty, F. M. Russell et al., Measurements on exotic atoms of helium, Nucl. Phys. A **392**, 297 (1983); [https://doi.org/10.1016/0375-9474\(83\)90127-6](https://doi.org/10.1016/0375-9474(83)90127-6).
- [44] R. J. Wetmore, D. C. Buckle, J. R. Kane, and R. T. Siegel, Pionic and muonic X rays in liquid helium, Phys. Rev. Lett. **19**, 1003 (1967); <https://doi.org/10.1103/PhysRevLett.19.1003>.
- [45] P. A. Souder, D. E. Casperson, T. W. Crane et al., Formation of the Muonic Helium Atom, $\alpha\mu^-e^-$, and Observation of Its Larmor Precession, Phys. Rev. Lett. **34**, 1417 (1975); <https://doi.org/10.1103/PhysRevA.22.33>.
- [46] G. Backenstoss, J. Egger, T. von Egidy et al., Pionic and muonic X-ray transitions in liquid helium, Nucl. Phys. A **232**, 519 (1974); [https://doi.org/10.1016/0375-9474\(74\)90637-X](https://doi.org/10.1016/0375-9474(74)90637-X).